

# Long-term trends in urban NO<sub>2</sub> concentrations and associated paediatric asthma incidence: estimates from global datasets



Susan C Anenberg\*, Arash Mohegh\*, Daniel L Goldberg, Gaige H Kerr, Michael Brauer, Katrin Burkart, Perry Hystad, Andrew Larkin, Sarah Wozniak, Lok Lamsal



## Summary

**Background** Combustion-related nitrogen dioxide (NO<sub>2</sub>) air pollution is associated with paediatric asthma incidence. We aimed to estimate global surface NO<sub>2</sub> concentrations consistent with the Global Burden of Disease study for 1990–2019 at a 1 km resolution, and the concentrations and attributable paediatric asthma incidence trends in 13 189 cities from 2000 to 2019.

**Methods** We scaled an existing annual average NO<sub>2</sub> concentration dataset for 2010–12 from a land use regression model (based on 5220 NO<sub>2</sub> monitors in 58 countries and land use variables) to other years using NO<sub>2</sub> column densities from satellite and reanalysis datasets. We applied these concentrations in an epidemiologically derived concentration–response function with population and baseline asthma rates to estimate NO<sub>2</sub>-attributable paediatric asthma incidence.

**Findings** We estimated that 1·85 million (95% uncertainty interval [UI] 0·93–2·80 million) new paediatric asthma cases were attributable to NO<sub>2</sub> globally in 2019, two thirds of which occurred in urban areas (1·22 million cases; 95% UI 0·60–1·8 million). The proportion of paediatric asthma incidence that is attributable to NO<sub>2</sub> in urban areas declined from 19·8% (1·22 million attributable cases of 6·14 million total cases) in 2000 to 16·0% (1·24 million attributable cases of 7·73 million total cases) in 2019. Urban attributable fractions dropped in high-income countries (–41%), Latin America and the Caribbean (–16%), central Europe, eastern Europe, and central Asia (–13%), and southeast Asia, east Asia, and Oceania (–6%), and rose in south Asia (+23%), sub-Saharan Africa (+11%), and north Africa and the Middle East (+5%). The contribution of NO<sub>2</sub> concentrations, paediatric population size, and asthma incidence rates to the change in NO<sub>2</sub>-attributable paediatric asthma incidence differed regionally.

**Interpretation** Despite improvements in some regions, combustion-related NO<sub>2</sub> pollution continues to be an important contributor to paediatric asthma incidence globally, particularly in cities. Mitigating air pollution should be a crucial element of public health strategies for children.

**Funding** Health Effects Institute, NASA.

**Copyright** © 2022 The Author(s). Published by Elsevier Ltd. This is an Open Access article under the CC BY-NC-ND 4.0 license.

## Introduction

Nitrogen dioxide (NO<sub>2</sub>), a component of nitrogen oxides, is a pervasive air pollutant that is a precursor to ground-level ozone and fine particulate matter (PM<sub>2.5</sub>), the leading contributors to air pollution-related mortality.<sup>1</sup> Major anthropogenic NO<sub>2</sub> sources include on-road and non-road transportation tailpipe emissions (including heavy, medium, and light duty vehicles, shipping, and aviation), power plants, industrial manufacturing, and agriculture.<sup>2–5</sup> NO<sub>2</sub> is an effective tracer for anthropogenic fuel combustion generally and traffic specifically, especially in urban areas.<sup>6–9</sup> NO<sub>2</sub> concentration trends can be used to evaluate the effectiveness of air pollution regulations, as well as the effects of abrupt emission changes (eg, power plant closures, new oil and gas fields, and COVID-19 lockdowns).<sup>10–14</sup>

Beyond its role in PM<sub>2.5</sub> and ozone formation, NO<sub>2</sub> itself has been associated with adverse health outcomes including asthma exacerbation.<sup>15,16</sup> Epidemiological studies

have also found associations between transportation-related air pollutants and new onset asthma in children.<sup>17,18</sup> Toxicological and gene environment research indicates that transportation-related air pollutants cause airway inflammation and remodelling due to oxidative stress, resulting in asthma development in some individuals.<sup>19</sup> Epidemiological studies are generally consistent in their finding that NO<sub>2</sub> is significantly associated with paediatric asthma incidence, whereas the evidence for other transportation-related air pollutants (eg, PM<sub>2.5</sub>) is more mixed.<sup>17,18</sup> Although the putative agent causing asthma in the traffic-related air pollution mixture is unknown, NO<sub>2</sub> could serve as a surrogate for other pollutants causing observed health effects. Previous health impact assessments have linked NO<sub>2</sub> with approximately 13% of the global paediatric asthma burden, and up to approximately 50% in the most populated 250 cities worldwide.<sup>19,20</sup>

Emission of nitrogen oxides and NO<sub>2</sub> concentrations have changed substantially in response to socioeconomic

*Lancet Planet Health* 2022; 6: e49–58

\*Contributed equally

Milken Institute School of Public Health, George Washington University, Washington, DC, USA (S C Anenberg PhD, A Mohegh PhD, D L Goldberg PhD, G H Kerr PhD); Energy Systems Division, Argonne National Laboratory, Washington, DC, USA (D L Goldberg); Institute for Health Metrics and Evaluation, University of Washington, Seattle, WA, USA (M Brauer ScD, K Burkart PhD, S Wozniak BS); University of British Columbia, Vancouver, BC, Canada (M Brauer); Oregon State University, Corvallis, OR, USA (P Hystad PhD, A Larkin PhD); NASA Goddard Space Flight Center, Greenbelt, MD, USA (L Lamsal PhD)

Correspondence to: Dr Susan C Anenberg, Milken Institute School of Public Health, George Washington University, Washington, DC 20052, USA [sanenberg@gwu.edu](mailto:sanenberg@gwu.edu)

## Research in context

### Evidence before this study

We searched PubMed and Google Scholar databases for studies published in English from the database inception until March 11, 2021, using the search terms (“NO<sub>2</sub>” OR “nitrogen dioxide”) AND “asthma” AND “trends”. Previous studies have reported epidemiological analyses linking changes in asthma incidence to changes in nitrogen dioxide (NO<sub>2</sub>) or have assessed long-term trends in NO<sub>2</sub> concentrations in some countries or world regions. However, these studies provide little information about how NO<sub>2</sub> concentrations are changing in urban areas all around the world, and the influence those changes have on paediatric asthma incidence. An earlier study published in 2019 showed that more than 4 million new paediatric asthma cases, representing approximately 13% of all paediatric asthma incidence worldwide in 2015, could be attributed to NO<sub>2</sub> pollution. Understanding temporal trends in NO<sub>2</sub>-attributable paediatric asthma incidence could help to inform asthma and air pollution mitigation strategies.

### Added value of this study

We show that urban areas have higher NO<sub>2</sub> concentrations and disease burdens compared with rural areas, with 16·4% of

paediatric asthma incidence in urban areas in 2019 estimated to be attributable to NO<sub>2</sub> pollution. We also find that the proportion of paediatric asthma incidence that is attributable to NO<sub>2</sub> declined in the high-income countries, Latin America and the Caribbean, and central Europe, eastern Europe, and central Asia from 2000 to 2019, and increased in the rest of the world, particularly in south Asia and sub-Saharan Africa. In doing this study, we produced the most spatially resolved (1 km × 1 km) long-term (1990–2019) dataset of surface NO<sub>2</sub> concentrations, which is compatible with the 2019 Global Burden of Disease Study and is now publicly available. Our study also shows the usefulness of satellite remote sensing for environmental and public health surveillance in urban areas worldwide.

### Implications of all the available evidence

Current concentrations of NO<sub>2</sub> contribute substantially to paediatric asthma incidence, particularly in cities. Mitigating air pollution should be a crucial element of children's public health strategies.

changes and regulation, even before the large-scale activity changes during the COVID-19 pandemic.<sup>21–25</sup> In the USA, average NO<sub>2</sub> concentrations dropped by approximately 50% from the 1980s to the 2010s,<sup>26</sup> with larger drops near major roadways<sup>26</sup> and point sources.<sup>10</sup> In the last two decades, nitrogen oxide emissions in the USA fell by 3–6% per year as vehicles became more fuel efficient and cleaner and power plants shifted from coal to relatively cleaner fuels (eg, natural gas).<sup>11,27,28</sup> NO<sub>2</sub> concentrations have also decreased in Europe, although more slowly.<sup>29,30</sup> In contrast, NO<sub>2</sub> has increased in India,<sup>31</sup> the Middle East,<sup>32</sup> and eastern Europe.<sup>23</sup> In China, nitrogen oxide emissions peaked around 2011 and 2012 and subsequently declined.<sup>33–35</sup>

NO<sub>2</sub> pollution is a paediatric health challenge in cities, driven by higher population growth, particularly in Asia and Africa where NO<sub>2</sub> concentrations have risen since 2000, and where there are higher asthma rates in cities compared with national averages.<sup>36</sup> Previous research on NO<sub>2</sub> temporal trends has focused on small subsets of cities and not considered its effects on health, precluding globally consistent comparisons of trends in NO<sub>2</sub> concentrations and the associated health burdens. The global coverage and the long continuous record of satellite remote sensing since the 1990s makes it possible to track NO<sub>2</sub> concentrations globally.<sup>37–40</sup> Additionally, the high spatial resolution of current satellites can capture NO<sub>2</sub> variation at urban and intra-urban scales,<sup>41,42</sup> although instrument performance has degraded by 3–8% between 2005 and 2016.<sup>43</sup>

Here we aimed to investigate the long-term trends of annual average NO<sub>2</sub> concentrations and associated

paediatric asthma burdens in 13 189 urban areas over the past two decades globally.

## Methods

### Overview

We first generated a new dataset of the annual average NO<sub>2</sub> concentration of the gridded global surface from 1990 to 2019 that is compatible with the spatiotemporal coverage of the Global Burden of Disease (GBD) 2019 study.<sup>1</sup> We then explored trends in NO<sub>2</sub> concentrations and attributable paediatric asthma incidence for urban areas from 2000 to 2019, for which the estimated concentrations have a greater certainty because of available ground monitoring. Finally, we deconstructed the drivers of these trends to explore the influence of NO<sub>2</sub> concentrations versus demographic changes. We integrated global environmental and demographic datasets from different sources to generate new estimates of surface NO<sub>2</sub> concentrations globally and NO<sub>2</sub>-attributable paediatric asthma incidence in cities. The analysis was done in Python (version 3.6.7).

### Globally gridded NO<sub>2</sub> concentrations

We generated a new dataset of surface annual average NO<sub>2</sub> concentrations at 0·0083° (~1 km<sup>2</sup>) resolution in 5-year increments from 1990 to 2010 and annually from 2010 to 2019, consistent with the years used in the unpublished GBD 2020 analysis. We used an existing global NO<sub>2</sub> concentration dataset (2010–12 average) at a 100 m resolution from a land use regression (LUR) model described by Larkin and colleagues<sup>44</sup> and made adjustments to correct for a high bias in rural areas and

to scale concentrations to additional years (appendix p 8). A full description of the methods and data sources used to construct the concentration dataset is in the appendix (pp 1–3).

For the base year 2011, we used the Larkin and colleagues<sup>44</sup> LUR estimates directly in all grid cells categorised as urban according to the Global Human Settlement Model grid<sup>45</sup> or that included major roadways. The LUR used annual measurements from 5220 air monitors in 58 countries (mostly in urban areas of Europe, North America, and Asia) with inputs from road networks, other land use variables, and satellite NO<sub>2</sub> column observations. Globally, the model captured 54% of NO<sub>2</sub> variation, with a mean absolute error of 3.7 parts per billion (ppb). Model performance differed regionally: the coefficient of determination (R<sup>2</sup>) varied from 0.42 in Africa to 0.67 in South America. In North America, Europe, and Asia, the R<sup>2</sup> (0.52 for each region) approximately matched the global average (0.54). For rural areas, we found that the Larkin and colleagues<sup>44</sup> dataset had NO<sub>2</sub> concentrations that were biased high, and therefore we adjusted concentrations using surface NO<sub>2</sub> concentrations derived from the Ozone Monitoring Instrument satellite NO<sub>2</sub> columns (appendix p 8). After adjusting the 2011 rural NO<sub>2</sub> concentration estimates, we scaled all 2011 grid cell concentrations to the GBD 2020 analysis period (1990–2019) using the Modern-Era Retrospective analysis for Research and Applications (version 2) reanalysis product<sup>46</sup> for 1990, 1995, and 2000, and the Ozone Monitoring Instrument NO<sub>2</sub> column densities for 2005–19 (appendix p 9).

Because Larkin and colleagues<sup>44</sup> showed that their NO<sub>2</sub> concentrations agreed well with the urban ground observations, we added evaluations of the changes made in this study. Firstly, we compared our 2011 rural NO<sub>2</sub> concentration estimates to the European Monitoring and Evaluation Programme ground monitoring dataset,<sup>47</sup> which has a large number of stations in rural areas, whereas rural monitors in other ground monitoring networks are often located directly downwind from urban areas. Secondly, we compared our 2019 NO<sub>2</sub> concentration estimates in urban and rural areas against 4348 monitors in the USA, Canada, and Europe.

Although we created this spatially (all urban and rural areas globally) and temporally (1990–2019) complete concentration dataset for compatibility with the GBD 2020 study, we focused our trend analysis on urban areas over the last two decades (2000–19), for which estimated concentrations have a greater certainty than previous decades because of available ground monitoring.

### NO<sub>2</sub>-attributable paediatric asthma incidence

We estimated the NO<sub>2</sub>-attributable cases of paediatric asthma incidence using a log linear concentration–response function that was epidemiologically derived,

following on from previous studies, using the equation:<sup>19,20</sup> See Online for appendix

$$\text{Burden}_{k,a} = \sum_{\substack{\text{Grid cells} \\ \text{in } k}} \text{Inc}_{c,a} \times \text{Pop}_{ij,a} \times (1 - e^{-\beta X_{ij}})$$

where Burden is the NO<sub>2</sub>-attributable asthma incidence in city *k* for age group *a*, Inc is the baseline asthma incidence rate for age group *a* and country *c*, Pop is the population in grid cell *i,j* for age group *a*,  $\beta$  is the concentration response factor relating the NO<sub>2</sub> concentration with increased risk of paediatric asthma incidence, and *X* is the annual average NO<sub>2</sub> concentration in grid cell *i,j*. We re-gridded all datasets to a 1 km resolution and estimated the NO<sub>2</sub>-attributable asthma incidence in each grid cell. We previously found that this resolution balances accuracy with computational efficiency in estimating city-level NO<sub>2</sub>-attributable disease burdens.<sup>20</sup> We summed up the results across all grid cells within each city for a city-level total.

We applied a relative risk of 1.26 (95% uncertainty interval [UI] 1.1–1.37) per 10 ppb annual average NO<sub>2</sub> concentration increase from a large epidemiological meta-analysis of 20 studies from Europe, 11 from North America, five from Japan, one from South Korea, and one from Taiwan. No regional heterogeneity was apparent in this meta-analysis, despite some variation in the relative risks reported in the underlying studies. We calculated the uncertainty in NO<sub>2</sub>-attributable paediatric asthma incidence using the statistical error in this relative risk estimate.<sup>17</sup> Because relative risk error is static over time, it does not influence temporal trends. We used a low concentration threshold of a less than 2 ppb annual average NO<sub>2</sub> concentration, the 5th percentile of the minimum concentrations reported by the studies in the meta-analysis. Alternative low concentration thresholds would not substantially affect the estimated trends in NO<sub>2</sub>-attributable asthma incidence, because thresholds were applied uniformly across all grid cells and only 3% of year-specific urban concentrations were less than 2 ppb.

We used population estimates from WorldPop<sup>48</sup> from 2000 to 2019 for ages 1–4, 5–9, 10–14, and 15–18 years at an approximately 1 km resolution, and summed up the results across age groups for total NO<sub>2</sub>-attributable paediatric asthma incidence. National baseline annual asthma incidence rates from 2000 to 2019 were obtained from the GBD 2019 study.<sup>1</sup> Urban area boundaries were obtained from the Global Human Settlement–Settlement Model grid Urban Centre dataset for 2015 (the latest year with available data at the time of analysis, applied here to all years).<sup>45</sup> We considered grid cells and in situ monitors (used to evaluate the concentration dataset) to be part of an urban cluster if they were located in urban and suburban areas in the Global Human Settlement–Settlement Model grid dataset (using a majority rule for grid cells), defined as areas with more than 300 people per km<sup>2</sup> that are part of clusters with more than 5000 people. All other grid

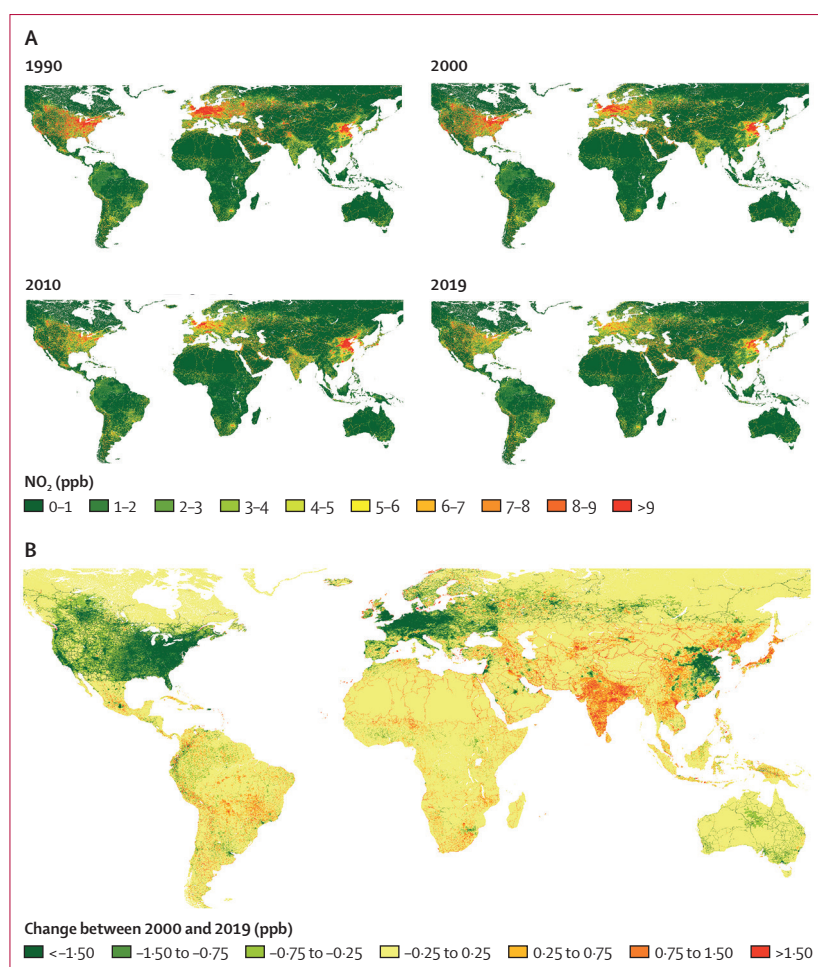


**Figure 1: Annual average NO<sub>2</sub> concentrations at a 1 km × 1 km resolution**  
Annual average NO<sub>2</sub> concentrations shown in 1990, 2000, 2010, and 2019 (A) and the difference in these concentrations between 2000 and 2019 (B). NO<sub>2</sub>=nitrogen dioxide. ppb=parts per billion.

cells and monitors were considered rural. World regions definitions were obtained from the GBD 2019 study (appendix pp 6, 10).<sup>1</sup>

### Drivers of change

To disentangle the drivers of temporal trends in NO<sub>2</sub>-attributable paediatric asthma incidence, we isolated the contribution of exposure, population size, and baseline asthma rates using the core results with annually varying data inputs, and three sets of simulations in which we reverted one contributing variable back to 2000 (appendix). Cohen and colleagues<sup>49</sup> used a similar approach for disentangling the drivers of national PM<sub>2.5</sub> disease burdens. We ignored interactions between the contributing factors (eg, the influence of changing NO<sub>2</sub> concentrations on baseline asthma rates), because we considered them to be minor relative to many other influences on these multi-factorial variables (eg, the effects of health-care advances on baseline asthma rates).

### Role of the funding source

The funders of the study had no role in study design, data collection, data analysis, data interpretation, or writing of the report.

### Results

Our new NO<sub>2</sub> concentration dataset reduces the rural high concentrations bias from the 2010–12 Larkin and colleagues<sup>44</sup> dataset (mean bias reduced from 2.4 to 1.0 ppb; appendix pp 5, 11) and captures the observed surface-level concentrations in both urban and rural areas in 2019 (mean bias 3.3 in Canada, 1.7 in the USA, and 2.3 in Europe; appendix p 12). See the appendix for further evaluation descriptions and results. Estimated NO<sub>2</sub> concentrations were highest in the most populated regions of the world, including North America, Europe, and south and east Asia throughout the time period (1990–2019; figure 1). The ten cities with the highest NO<sub>2</sub> concentrations in 2019 were located in the Middle East (Lebanon, Iraq, and Iran), China, and Russia (appendix p 13).

We estimated that the average annual mean NO<sub>2</sub> concentration, weighted by the global population, was 6.6 ppb (~12.4 µm<sup>3</sup> assuming a 1 standard atmosphere ambient pressure at 25° C) in 2019, leading to 1.85 million (95% UI 0.93–2.80 million) new asthma cases among children worldwide that year, or 8.5% (95% UI 4.3–12.8%; 1.85 million attributable cases of 21.78 million total cases) of all paediatric asthma incidence (figure 2). Approximately two thirds of NO<sub>2</sub>-attributable paediatric asthma incidence occurred in the 13189 urban areas (1.22 million cases; 95% UI 0.60–1.79 million). Compared with rural areas, urban areas had 2–4 times higher population-weighted NO<sub>2</sub> concentrations (10.6 ppb in urban areas vs 4.2 ppb in rural areas), NO<sub>2</sub>-attributable asthma cases (1.22 million [95% CI 0.60–1.79 million] in urban areas vs 0.63 million [0.33–0.99 million] in rural areas), NO<sub>2</sub>-attributable asthma cases per 100 000 people (156 [77–228] in urban areas vs 40 [21–63] in rural areas), and attributable proportions (16.4% in urban areas vs 4.5% in rural areas) in 2019.

Focusing on urban areas in the last two decades (2000–19), we found that annual average NO<sub>2</sub> concentrations decreased by 13%, from 12.2 ppb in 2000 to 10.6 ppb in 2019, with a steady decline from 2011 to 2019 after rising from 2000 to 2011 (figure 2). NO<sub>2</sub> concentrations in high-income cities exceeded the global average throughout the time period, despite declining 38% from 17.6 ppb in 2000 to 11.0 ppb in 2019 (figure 3). Contrastingly, concentrations rose by 18% (from 8.6 to 10.1 ppb) in south Asia and 11% (from 6.4 to 7.1 ppb) in sub-Saharan Africa, but were lower than the global urban average throughout the time period. These large regional groupings of cities obscure contrasting trends between sub-regions in some cases (appendix p 14).

We estimated that approximately 1.2 million paediatric asthma cases in urban areas globally were



attributable to NO<sub>2</sub> pollution in both 2000 and 2019, although the rate per 100 000 children declined by 11% from 176 to 156 per 100 000 children as the urban paediatric population grew by 14% (from 679 million to 774 million; figure 2). High-income cities had the most NO<sub>2</sub>-attributable asthma incidence in 2019, with 340 900 cases or 28% of the global urban total, despite having only 14% (110 million of 774 million) of the global urban paediatric population (figure 4; appendix p 7). Although the majority of the total NO<sub>2</sub>-attributable paediatric asthma cases were in the most populated cities in the world (appendix p 15), all ten highest attributable rates were in US cities (appendix p 16). Contrastingly, cities in south Asia, with approximately a quarter of the global paediatric population, only accounted for 7% (90 400 cases) of global urban NO<sub>2</sub>-attributable paediatric asthma incidence. NO<sub>2</sub>-attributable paediatric asthma incidence rates were also highest in the high-income region (310 attributable cases per 100 000 children; figure 3 and appendix p 7) and were an order of magnitude lower in south Asia (50 attributable cases in south Asia).

The proportion of paediatric asthma incidence that were estimated to be attributable to NO<sub>2</sub> across all urban areas globally dropped from 19·8% (1·22 million attributable cases of 6·14 million total cases) in 2000 to 16·0% (1·24 million attributable cases of 7·73 million total cases) in 2019 (figure 2). Urban attributable fractions dropped between 2000 and 2019 in high-income countries (–41%), Latin America and the Caribbean (–16%), central Europe, eastern Europe, and central Asia (–13%), and southeast Asia, east Asia, and Oceania (–6%), and rose in south Asia (+23%), sub-Saharan Africa (+11%), and north Africa and the Middle East (+5%; figure 3 and appendix p 7). The large decrease in high-income countries is partly driven by even larger drops in North America (–52%; appendix p 14). The 13% decrease in central Europe, eastern Europe, and central Asia was driven by a 24% increase in central Asia, balanced by a 32% decrease in central Europe and a 16% decrease in eastern Europe. In 2019, the regional urban average attributable fractions ranged from 10% (102 900 attributable cases of 1·05 million total cases) in sub-Saharan Africa to 20% (54 900 attributable cases of 277 800 total cases) in central Europe, eastern Europe, and central Asia, and north Africa and the Middle East. As for concentrations, the ten highest attributable fractions were located in Lebanon, Iraq, Iran, China, and Russia (appendix p 17).

Estimated temporal trends in urban NO<sub>2</sub>-attributable paediatric asthma incidence are driven by simultaneous and often competing changes in NO<sub>2</sub> concentrations, paediatric population, and asthma incidence rates (figure 5). Australasia and high-income Asia-Pacific were the only regions where declining concentrations, paediatric population size, and asthma rates all contributed to overall drops in NO<sub>2</sub>-attributable paediatric asthma incidence. The

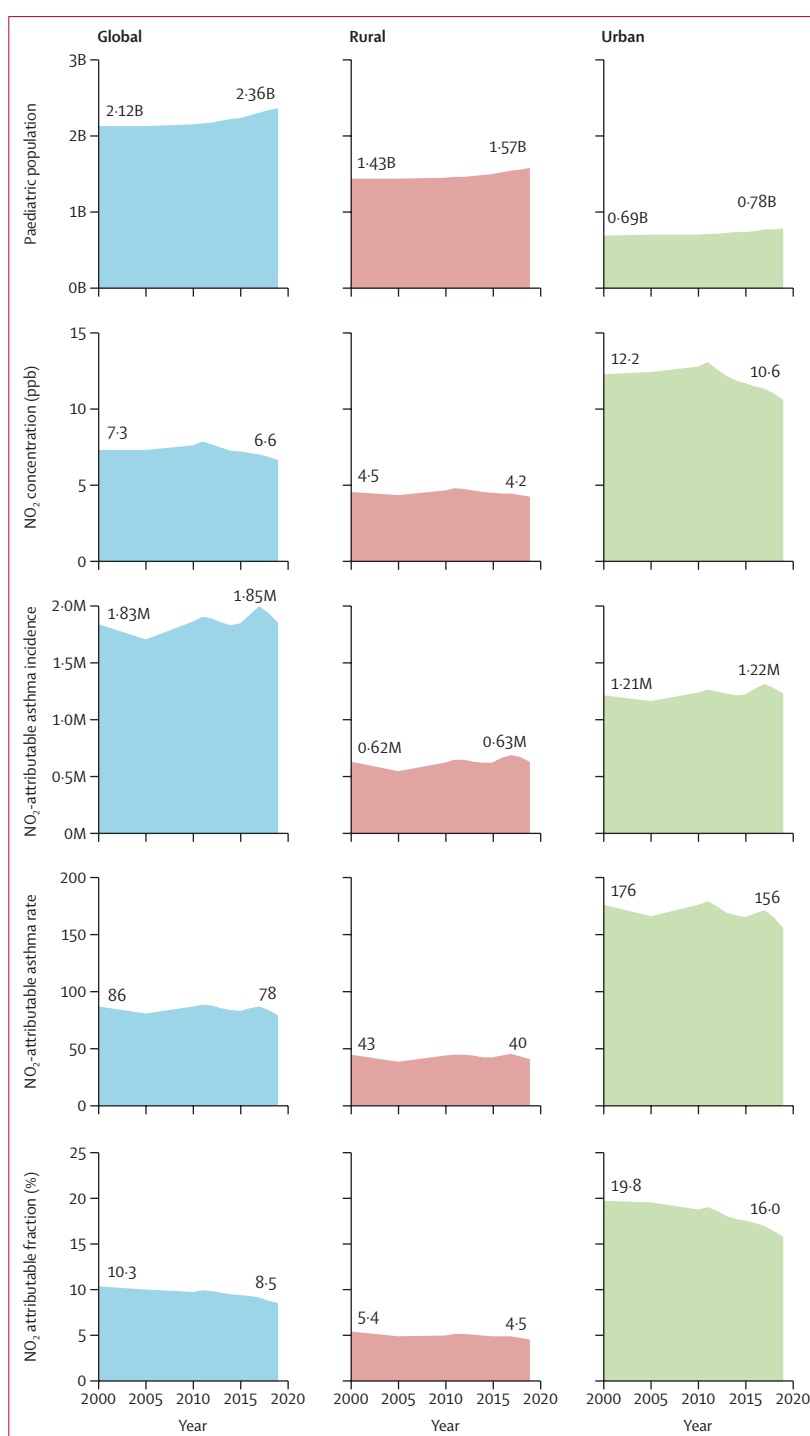


**Figure 2: Trends between 2000 and 2019 globally and in urban and rural areas**

The paediatric population, the population-weighted annual average NO<sub>2</sub> concentrations (ppb), NO<sub>2</sub>-attributable paediatric asthma incidence (number of cases), NO<sub>2</sub>-attributable paediatric asthma incidence rate (per 100 000 children), and NO<sub>2</sub> attributable fraction (% of all paediatric asthma incidence) globally, in all rural areas, and in 13 189 urban areas are shown. The uncertainty intervals for NO<sub>2</sub>-attributable paediatric asthma incidence are not shown since they are based on error in the relative risk estimate, which is constant over time. B=billion. M=million. NO<sub>2</sub>=nitrogen dioxide. ppb=parts per billion.

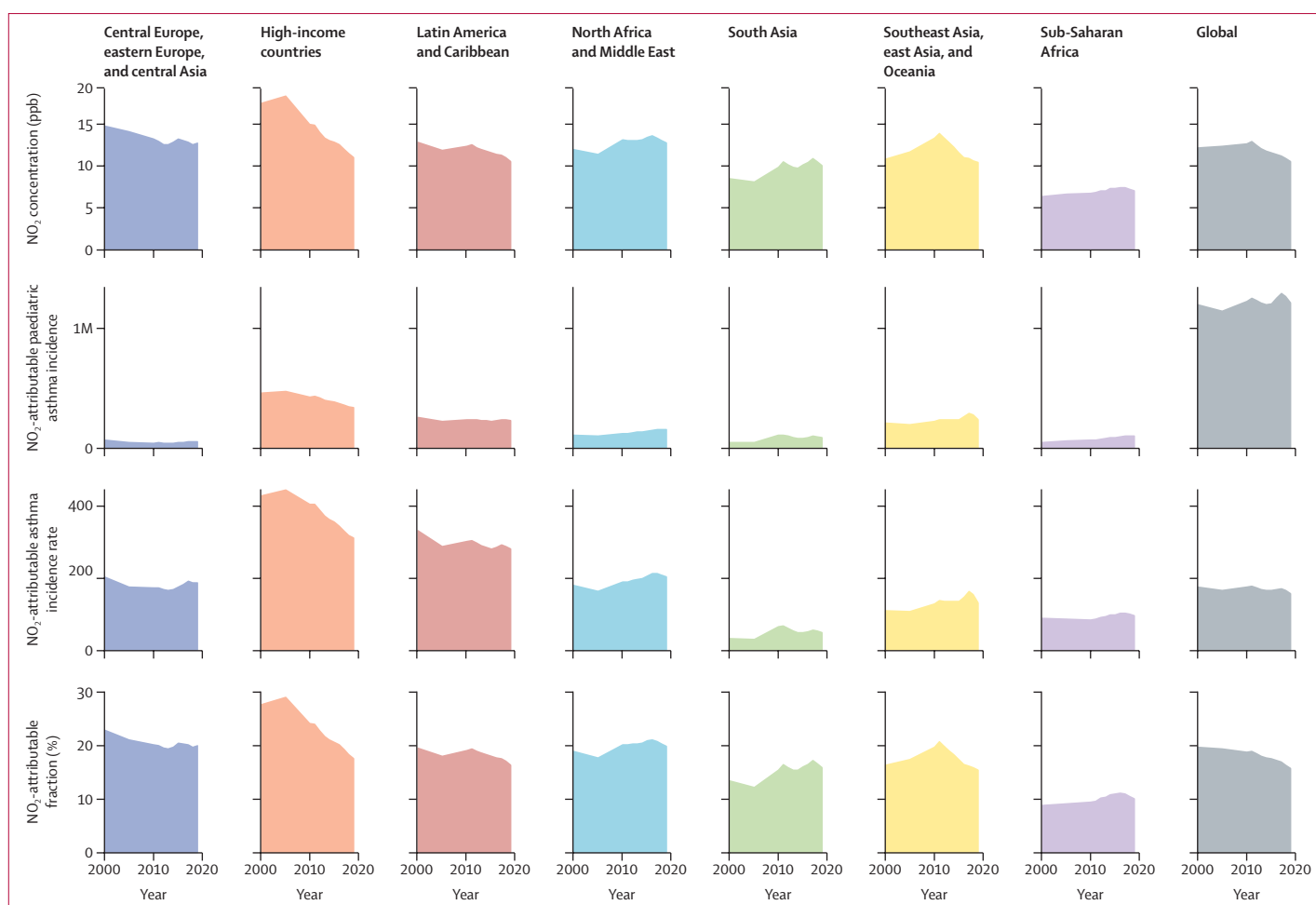


**Figure 3: Trends between 2000 and 2019 in urban areas by region**

Population-weighted annual average  $\text{NO}_2$  concentrations (ppb),  $\text{NO}_2$ -attributable paediatric asthma incidence (number of cases),  $\text{NO}_2$ -attributable paediatric asthma rates (per 100 000 children), and  $\text{NO}_2$ -attributable fraction (% of all paediatric asthma incidence) in urban areas in each region are shown. Results for each sub-region within each super-region are shown in the appendix (p 14). Uncertainty intervals for  $\text{NO}_2$ -attributable paediatric asthma incidence are not shown since they are based on error in the relative risk estimate, which is constant over time. M=million.  $\text{NO}_2$ =nitrogen dioxide. ppb=parts per billion.

opposite occurred in central, south, and southeast Asia, and in north Africa and the Middle East, where concentrations, paediatric population, and asthma rates all rose. In high-income North America, western, eastern, and central Europe, southern, central, tropical, and Andean Latin America, east Asia, and central sub-Saharan Africa, declining  $\text{NO}_2$  concentrations were offset by increases in asthma incidence rates or paediatric population size, or both. These competing influences changed over time, with declining concentrations becoming more influential over time in North America and southern Latin America, and population growth becoming more influential in north Africa and the Middle East and southern sub-Saharan Africa (appendix p 18).

## Discussion

We estimated that 1·85 million (95% UI 0·93–2·80 million) paediatric asthma cases globally could be attributable to

$\text{NO}_2$  pollution in 2019. Despite having only a third of the global paediatric population, urban areas had two thirds of  $\text{NO}_2$ -attributable paediatric asthma incidence. The  $\text{NO}_2$ -attributable fraction of paediatric asthma incidence in urban areas globally declined from 19·8% in 2000 to 16·0% in 2019. Regional trends were inconsistent: urban average attributable fractions dropped in high-income countries, Latin America and the Caribbean, central and eastern Europe, central, southeast, and east Asia, and Oceania, and rose in south Asia, sub-Saharan Africa, and north Africa and the Middle East. The drivers of temporal trends in  $\text{NO}_2$  concentrations and paediatric asthma burdens were also inconsistent regionally, with declining  $\text{NO}_2$  concentrations in some regions counteracted by increases in paediatric population size and asthma incidence rates.

Our study is consistent with the broader literature showing that  $\text{NO}_2$  is largely an urban pollutant.<sup>7,50–52</sup>

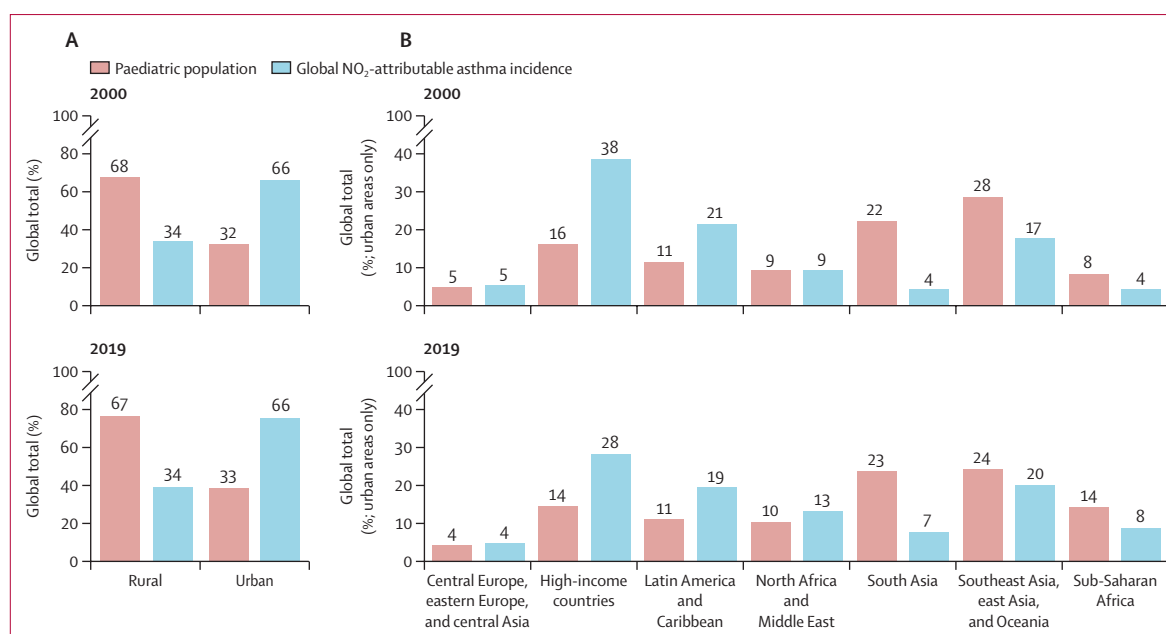


**Figure 4: Percentage of global total paediatric population and NO<sub>2</sub>-attributable asthma cases in 2000 and 2019**

Percentage of global total paediatric population and NO<sub>2</sub>-attributable asthma cases in all rural areas and 13 189 urban areas globally (A), and urban areas only within each region (B). NO<sub>2</sub>=nitrogen dioxide.

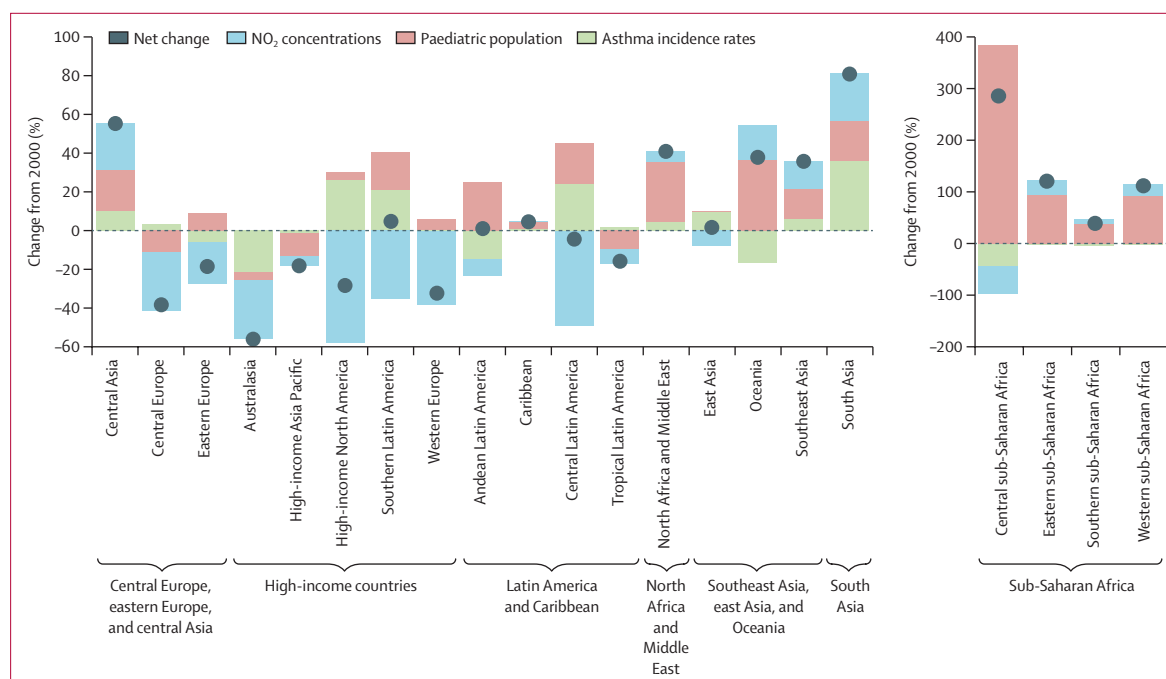


**Figure 5: Contribution of paediatric population, baseline paediatric asthma rates, and NO<sub>2</sub> concentrations to the changes in estimated NO<sub>2</sub>-attributable paediatric asthma incidence between 2000 and 2019 for each sub-region**

A different y-axis is used for regions in sub-Saharan Africa, as shown in the figure. Results for the full time period are shown in the appendix (p 18). NO<sub>2</sub>=nitrogen dioxide.

Estimated NO<sub>2</sub> concentration trends are consistent with studies using satellite data to investigate NO<sub>2</sub> concentration trends during 2004–18 for the USA, Europe, China, India, and Japan.<sup>23,31,53</sup> For example, Qu and colleagues<sup>54</sup> also

showed a similar decrease in US NO<sub>2</sub> concentrations based on ground observations, satellite data, and modelling outputs from 2006 to 2016, and Henneman and colleagues<sup>26</sup> showed a similar decrease using ground

observations from 1980 to 2020. One study focused on biomass burning in the equatorial Africa region found declining concentrations in NO<sub>2</sub> from 2005 to 2017,<sup>55</sup> whereas we found an increase in sub-Saharan Africa from 2000 to 2019. A biomass burning decline in the region might be smaller and offset by anthropogenic emission changes in populated urban areas. A reduced effect on asthma where NO<sub>2</sub> concentrations are declining is consistent with observational studies.<sup>56</sup>

Although our new NO<sub>2</sub> dataset leverages the advantages of having different data sources, the concentrations are still uncertain. Many cities, particularly in low-income and middle-income countries (LMICs), do not have ground NO<sub>2</sub> monitors, challenging the calibration and evaluation of LUR models.<sup>44</sup> Urban NO<sub>2</sub> concentrations are therefore more certain in North America, Europe, and Asia compared with Africa and south America. Rural concentrations are uncertain globally with little ground monitoring outside of urban areas. Scaling the 2010–12 LUR NO<sub>2</sub> concentrations to other years assumes that the land use predictors are static over time. This assumption is likely to be supported by slow changes in road density and volume and urban form, but over the two decades explored here, some land use evolution is probable,<sup>57</sup> particularly in rapidly developing LMICs. The actual relationships between land use variables and NO<sub>2</sub> concentrations probably differ temporally, and holding these variables constant results in greater uncertainties in NO<sub>2</sub> concentrations in areas where land use is changing rapidly. The directional effect of these uncertainties on the results is unknown.

Our estimate of the global burden of NO<sub>2</sub> on paediatric asthma incidence in 2019 is less than half of the 4·2 million found by Achakulwisut and colleagues<sup>19</sup> in 2015. Our results for India are also lower than previous estimates, whereas our results for the USA are higher.<sup>17,20</sup> Several factors explain this discrepancy. First, our new NO<sub>2</sub> concentrations correct for a high rural NO<sub>2</sub> bias, leading to lower NO<sub>2</sub>-attributable asthma incidence estimates, especially in countries with larger rural populations (eg, India). Second, the GBD 2019 study baseline asthma rates are much lower than in previous versions, except in high-income areas (eg, the USA), because of a change in the case definition used that lowered the estimated rates in most places and raised them for the USA.<sup>58</sup> For example, baseline paediatric asthma incidence rates in 2015 (the year analysed by Mohegh and colleagues<sup>20</sup>) in the GBD 2019 study were 81% of the GBD 2017 study values. Contrastingly, US paediatric asthma incidence rates were 2·2 times higher in the GBD 2019 study versus the GBD 2017 study. Changes in baseline asthma rates approximately affect estimated NO<sub>2</sub>-attributable paediatric asthma incidence. Our NO<sub>2</sub> attributable fraction result in high-income North America in 2019 (17·3%) was similar to a previous estimate for the USA in 2000 (17·9%), although our NO<sub>2</sub> concentrations were lower than the

previous study (10·9 ppb in urban areas vs 13·2 ppb overall).<sup>50</sup> The different analysis years are important because, as we have shown, NO<sub>2</sub> concentrations trends are changing rapidly.

The health impact assessment method also introduces uncertainties. Baseline paediatric asthma incidence rates might be underestimated in many LMICs, leading to underestimated NO<sub>2</sub>-attributable asthma effects. Additionally, although we used national paediatric asthma rates because city-level rates are unavailable globally, asthma prevalence varies within countries.<sup>50</sup> Living in urban areas has been associated with an increased risk of asthma prevalence in LMICs<sup>56</sup> and asthma-related emergency department visits and admissions to hospital in the USA.<sup>59</sup> Similarly, temporal trends in baseline asthma incidence might differ in urban areas compared with national averages, especially in rapidly urbanising LMICs. If asthma prevalence is higher in urban areas compared with national averages, NO<sub>2</sub>-attributable asthma incidence might be underestimated. Temporal trends could also be affected by changing population structure, health-care levels, and other factors that we have not attempted to quantify here. In addition, it is currently unknown whether paediatric asthma incidence is directly associated with NO<sub>2</sub>, or with the traffic-related air pollution mixture or the broader combustion-related air pollution mixture. Our results could be affected by exposure misclassification, which would tend to lead to bias towards the null and underestimated attributable asthma effects. Similarly, we have not accounted for various factors that influence the ambient NO<sub>2</sub>-asthma relationship in the underlying epidemiological studies and meta-analysis from which we drew relative risk estimates (effect modification). These include parental income and educational levels, environmental tobacco smoke, and presence in the home of mildew, water damage, pests, and pets. Since we held urban area boundaries constant over the time period examined, we were not able to associate NO<sub>2</sub>-attributable asthma changes with the evolving urban area. Finally, the 1 km resolution of our NO<sub>2</sub> concentration estimates might not capture areas with co-located steep spatial gradients in concentrations and population, potentially leading NO<sub>2</sub>-attributable asthma incidence to be underestimated.

Despite these uncertainties and limitations, our results show the important influence of combustion-related air pollution on children's health in cities globally. In places that have effective air quality management programmes (eg, in the USA and Europe), NO<sub>2</sub> concentrations have been trending downward for decades, with benefits for children's respiratory health. Even with these improvements, current NO<sub>2</sub> concentrations contribute substantially to paediatric asthma incidence, highlighting that mitigating air pollution should be a crucial element of public health strategies for children. For cities that have not benefited from strong air quality management programmes at the local or national scale, the experience



of cities that have such programmes shows that addressing combustion-related air pollution can lead to major air quality and public health improvements over short time frames. These air quality improvements can be achieved through either end-of-pipe emission control technologies such as catalytic converters or avoiding the combustion in the first place, which would have additional benefits from reduced greenhouse gas emissions.

Our study shows the value of satellite remote sensing and statistical models for tracking NO<sub>2</sub> pollution and for environmental health surveillance at local, national, and global scales. The combination of methods offers strengths beyond the capabilities of each technique alone: a long and consistent observational record of NO<sub>2</sub> column densities from satellites in combination with the high spatial resolution of surface concentration predictions from LUR models. Future studies might leverage these data sources and others, including new satellite sensors that have higher temporal and spatial resolutions, mobile monitoring, distributed ground sensor networks, and chemical transport models, to further improve the accuracy and spatiotemporal resolution of NO<sub>2</sub> concentration estimates, which can be used in both epidemiological studies and health impact assessments. Further, our study shows the importance of considering demographic changes over time for understanding air pollution health risks. Improved and more widely accessible information about disease rates, and capturing population distribution and movement, will enable more accurate and highly resolved air pollution health impact assessments.

#### Contributors

SCA, AM, and DLG designed the study. PH, AL, and LL provided data. AM and GHK carried out the calculations. SCA, AM, DLG, KB, MB, PH, AL, and SW contributed input on methods development. SCA and AM wrote the paper. All authors helped interpret the results and reviewed the paper. AM, GHK, and DLG have verified the underlying data. AM, GHK, DLG, and SCA had full access to all data in the study. SCA and AM had final responsibility for the decision to submit for publication.

#### Declaration of interests

GHK declares a consulting relationship with the Environmental Defense Fund. SCA declares consulting relationships with the Environmental Defense Fund and International Council on Clean Transportation; and unpaid advisory board membership for the American Geophysical Union, US Environmental Protection Agency, WHO, Clean Air Partners, and the National Academies of Sciences, outside the submitted work. All other authors declare no competing interests.

#### Data sharing

The NO<sub>2</sub> concentrations are available at: <https://doi.org/10.6084/m9.figshare.12968114>. The estimated NO<sub>2</sub>-attributable asthma incidence results are available at: <https://blogs.gwu.edu/sanenbergh/>.

#### Acknowledgments

This study was supported by grants from the Health Effects Institute and Bloomberg Philanthropies (research agreement 4977/20–11) and NASA (grant number 80NSSC19K0193). We acknowledge the developers of the Ozone Monitoring Instrument NO<sub>2</sub> concentration products, Global Human Settlement–Settlement Model grid urban area dataset, Global Burden of Disease rate datasets, and WorldPop population dataset. We appreciate helpful discussions with Bryan Duncan. The contents of this Article do not necessarily reflect the views of the Health Effects Institute, or its sponsors.

Editorial note: the *Lancet* Group takes a neutral position with respect to territorial claims in published maps and institutional affiliations.

#### References

- 1 Murray CJL, Aravkin AY, Zheng P, et al. Global burden of 87 risk factors in 204 countries and territories, 1990–2019: a systematic analysis for the Global Burden of Disease Study 2019. *Lancet* 2020; **396**: 1223–49.
- 2 McDuffie EE, Smith SJ, O'Rourke P, et al. A global anthropogenic emission inventory of atmospheric pollutants from sector- and fuel-specific sources (1970–2017): an application of the Community Emissions Data System (CEDS). *Earth Syst Sci Data* 2020; **12**: 3413–42.
- 3 Anenberg SC, Miller J, Minjares R, et al. Impacts and mitigation of excess diesel-related NO<sub>x</sub> emissions in 11 major vehicle markets. *Nature* 2017; **545**: 467–71.
- 4 Stohl A, Aamaas B, Amann M, et al. Evaluating the climate and air quality impacts of short-lived pollutants. *Atmos Chem Phys* 2015; **15**: 10529–66.
- 5 Crippa M, Guizzardi D, Muntean M, et al. Gridded emissions of air pollutants for the period 1970–2012 within EDGAR v4.3.2. *Earth Syst Sci Data* 2018; **10**: 1987–2013.
- 6 Stavrakou T, Müller J-F, Boersma KF, De Smedt I, van der A RJ. Assessing the distribution and growth rates of NO<sub>x</sub> emission sources by inverting a 10-year record of NO<sub>x</sub> satellite columns. *Geophys Res Lett* 2008; **35**: L10801.
- 7 Bechle MJ, Millet DB, Marshall JD. Effects of income and urban form on urban NO<sub>2</sub>: global evidence from satellites. *Environ Sci Technol* 2011; **45**: 4914–19.
- 8 Geddes JA, Martin RV, Boys BL, van Donkelaar A. Long-term trends worldwide in ambient NO<sub>2</sub> concentrations inferred from satellite observations. *Environ Health Perspect* 2016; **124**: 281–89.
- 9 Bechle MJ, Millet DB, Marshall JD. Does urban form affect urban NO<sub>2</sub>? Satellite-based evidence for more than 1200 cities. *Environ Sci Technol* 2017; **51**: 12707–16.
- 10 Duncan BN, Yoshida Y, de Foy B, et al. The observed response of Ozone Monitoring Instrument (OMI) NO<sub>2</sub> columns to NO<sub>x</sub> emission controls on power plants in the United States: 2005–2011. *Atmos Environ* 2013; **81**: 102–11.
- 11 Silvern RF, Jacob DJ, Mickley LJ, et al. Using satellite observations of tropospheric NO<sub>2</sub> columns to infer long-term trends in US NO<sub>x</sub> emissions: the importance of accounting for the free tropospheric NO<sub>2</sub> background. *Atmos Chem Phys* 2019; **19**: 8863–78.
- 12 Dix B, Bruin J, Roosenbrand E, et al. Nitrogen oxide emissions from U.S. oil and gas production: recent trends and source attribution. *Geophys Res Lett* 2020; **47**: e2019GL085866.
- 13 Goldberg DL, Anenberg SC, Griffin D, McLinden CA, Lu Z, Streets DG. Disentangling the impact of the COVID-19 lockdowns on urban NO<sub>2</sub> from natural variability. *Geophys Res Lett* 2020; **47**: GL089269.
- 14 Kerr GH, Goldberg DL, Anenberg SC. COVID-19 pandemic reveals persistent disparities in nitrogen dioxide pollution. *Proc Natl Acad Sci USA* 2021; **118**: e2022409118.
- 15 Perez L, Lurmann F, Wilson J, et al. Near-roadway pollution and childhood asthma: implications for developing “win-win” compact urban development and clean vehicle strategies. *Environ Health Perspect* 2012; **120**: 1619–26.
- 16 Gauderman WJ, Avol E, Lurmann F, et al. Childhood asthma and exposure to traffic and nitrogen dioxide. *Epidemiology* 2005; **16**: 737–43.
- 17 Khreis H, Kelly C, Tate J, Parslow R, Lucas K, Nieuwenhuijsen M. Exposure to traffic-related air pollution and risk of development of childhood asthma: a systematic review and meta-analysis. *Environ Int* 2017; **100**: 1–31.
- 18 Anenberg SC, Henze DK, Tinney V, et al. Estimates of the global burden of ambient PM<sub>2.5</sub>, ozone, and NO<sub>2</sub> on asthma incidence and emergency room visits. *Environ Health Perspect* 2018; **126**: 107004.
- 19 Achakulwisut P, Brauer M, Hystad P, Anenberg SC. Global, national, and urban burdens of paediatric asthma incidence attributable to ambient NO<sub>2</sub> pollution: estimates from global datasets. *Lancet Planet Health* 2019; **3**: e166–78.
- 20 Mohegheh A, Goldberg D, Achakulwisut P, Anenberg SC. Sensitivity of estimated NO<sub>2</sub>-attributable pediatric asthma incidence to grid resolution and urbanicity. *Environ Res Lett* 2020; **16**: 014019.

- 21 Lamsal LN, Duncan BN, Yoshida Y, et al. NO<sub>2</sub> trends (2005–2013): EPA Air Quality System (AQS) data versus improved observations from the Ozone Monitoring Instrument (OMI). *Atmos Environ* 2015; **110**: 130–43.
- 22 Miyazaki K, Eskes H, Sudo K, Boersma KF, Bowman K, Kanaya Y. Decadal changes in global surface NO<sub>x</sub> emissions from multi-constituent satellite data assimilation. *Atmos Chem Phys* 2017; **17**: 807–37.
- 23 Georgoulias AK, van der A RJ, Stammes P, Boersma KF, Eskes HJ. Trends and trend reversal detection in 2 decades of tropospheric NO<sub>2</sub> satellite observations. *Atmos Chem Phys* 2019; **19**: 6269–94.
- 24 Tong DQ, Lamsal L, Pan L, et al. Long-term NO<sub>x</sub> trends over large cities in the United States during the great recession: comparison of satellite retrievals, ground observations, and emission inventories. *Atmos Environ* 2015; **107**: 70–84.
- 25 Kharol SK, Martin RV, Philip S, et al. Assessment of the magnitude and recent trends in satellite-derived ground-level nitrogen dioxide over North America. *Atmos Environ* 2015; **118**: 236–45.
- 26 Henneman LRF, Shen H, Hogrefe C, Russell AG, Zigler CM. Four decades of United States mobile source pollutants: spatial-temporal trends assessed by ground-based monitors, air quality models, and satellites. *Environ Sci Technol* 2021; **55**: 882–92.
- 27 Goldberg DL, Lu Z, Oda T, et al. Exploiting OMI NO<sub>2</sub> satellite observations to infer fossil-fuel CO<sub>2</sub> emissions from U.S. megacities. *Sci Total Environ* 2019; **695**: 133805.
- 28 Zhang R, Wang Y, Smeltzer C, Qu H, Koshak W, Boersma KF. Comparing OMI-based and EPA AQS in situ NO<sub>2</sub> trends: towards understanding surface NO<sub>x</sub> emission changes. *Atmos Meas Tech* 2018; **11**: 3955–67.
- 29 Curier RL, Kranenburg R, Segers AJS, Timmermans RMA, Schaap M. Synergistic use of OMI NO<sub>2</sub> tropospheric columns and LOTOS–EUROS to evaluate the NO<sub>x</sub> emission trends across Europe. *Remote Sens Environ* 2014; **149**: 58–69.
- 30 Zara M, Boersma KF, Eskes H, et al. Reductions in nitrogen oxides over the Netherlands between 2005 and 2018 observed from space and on the ground: decreasing emissions and increasing O<sub>3</sub> indicate changing NO<sub>x</sub> chemistry. *Atmos Environ X* 2021; **9**: 100104.
- 31 Itahashi S, Yumimoto K, Kurokawa J, et al. Inverse estimation of NO<sub>x</sub> emissions over China and India 2005–2016: contrasting recent trends and future perspectives. *Environ Res Lett* 2019; **14**: 124020.
- 32 Barkley MP, González Abad G, Kurosu TP, Spurr R, Torbatian S, Lerot C. OMI air-quality monitoring over the Middle East. *Atmos Chem Phys* 2017; **17**: 4687–709.
- 33 de Foy B, Lu Z, Streets DG. Satellite NO<sub>2</sub> retrievals suggest China has exceeded its NO<sub>2</sub> reduction goals from the twelfth five-year plan. *Sci Rep* 2016; **6**: 35912.
- 34 Liu F, Beirle S, Zhang Q, et al. NO<sub>x</sub> emission trends over Chinese cities estimated from OMI observations during 2005 to 2015. *Atmos Chem Phys* 2017; **17**: 9261–75.
- 35 Zheng B, Tong D, Li M, et al. Trends in China's anthropogenic emissions since 2010 as the consequence of clean air actions. *Atmos Chem Phys* 2018; **18**: 14095–111.
- 36 Rodriguez A, Brickley E, Rodrigues L, Normansell RA, Barreto M, Cooper PJ. Urbanisation and asthma in low-income and middle-income countries: a systematic review of the urban-rural differences in asthma prevalence. *Thorax* 2019; **74**: 1020–30.
- 37 Leue C, Wenig M, Wagner T, Klimm O, Platt U, Jähne B. Quantitative analysis of NO<sub>x</sub> emissions from global ozone monitoring experiment satellite image sequences. *J Geophys Res* 2001; **106**: 5493–505.
- 38 van der A RJ, Eskes HJ, Boersma KF. Trends, seasonal variability and dominant NO<sub>x</sub> source derived from a ten year record of NO<sub>2</sub> measured from space. *J Geophys Res* 2008; **113**: D04302.
- 39 Duncan BN, Lamsal LN, Thompson AM, et al. Space-based, high-resolution view of notable changes in urban NO<sub>x</sub> pollution around the world (2005–2014). *J Geophys Res Atmos* 2016; **121**: 976–96.
- 40 Anenberg SC, Bindl M, Brauer M, et al. Using satellites to track indicators of global air pollution and climate change impacts: lessons learned from a NASA-supported science-stakeholder collaborative. *Gehealth* 2020; **4**: GH000270.
- 41 Griffin D, McLinden CA, Boersma F, et al. High resolution mapping of nitrogen dioxide with TROPOMI: first results and validation over the Canadian oil sands. *Geophys Res Lett* 2019; **46**: 1049–60.
- 42 Goldberg DL, Anenberg SC, Kerr GH, Moheggh A, Lu Z, Streets DG. TROPOMI NO<sub>2</sub> in the United States: a detailed look at the annual averages, weekly cycles, effects of temperature, and correlation with surface NO<sub>2</sub> concentrations. *Earths Futur* 2021; **9**: EF001665.
- 43 Schenkeveld VME, Jaross G, Marchenko S, et al. In-flight performance of the Ozone Monitoring Instrument. *Atmos Meas Tech* 2017; **10**: 1957–86.
- 44 Larkin A, Geddes JA, Martin RV, et al. Global land use regression model for nitrogen dioxide air pollution. *Environ Sci Technol* 2017; **51**: 6957–64.
- 45 Pesaresi M, Florczyk A, Schiavina M, Melchiorri M, Maffineni L. GHS-SMOD R2019A - GHS settlement layers, updated and refined REGIO model 2014 in application to GHS-BUILT R2018A and GHS-POP R2019A, multitemporal (1975-1990-2000-2015). 2019. <https://data.jrc.ec.europa.eu/dataset/42e8be89-54ff-464e-be7b-bf9e64da5218> (accessed Feb 1, 2019).
- 46 Gelaro R, McCarty W, Suárez MJ, et al. The Modern-Era Retrospective analysis for Research and Applications, version 2 (MERRA-2). *J Clim* 2017; **30**: 5419–54.
- 47 European Environment Agency. Air quality e-reporting (AQ e-reporting). Sept 30, 2021. <https://www.eea.europa.eu/data-and-maps/data/aqereporting-9> (accessed May 5, 2020).
- 48 Tatem AJ. WorldPop, open data for spatial demography. *Sci Data* 2017; **4**: 170004.
- 49 Cohen AJ, Brauer M, Burnett R, et al. Estimates and 25-year trends of the global burden of disease attributable to ambient air pollution: an analysis of data from the Global Burden of Diseases Study 2015. *Lancet* 2017; **389**: 1907–18.
- 50 Khreis H, Alotaibi R, Horney J, McConnell R. The impact of baseline incidence rates on burden of disease assessment of air pollution and onset childhood asthma: analysis of data from the contiguous United States. *Ann Epidemiol* 2021; **53**: 76–88.e10.
- 51 Bechle MJ, Millet DB, Marshall JD. National spatiotemporal exposure surface for NO<sub>2</sub>: monthly scaling of a satellite-derived land-use regression, 2000-2010. *Environ Sci Technol* 2015; **49**: 12297–305.
- 52 Lee HJ, Koutrakis P. Daily ambient NO<sub>2</sub> concentration predictions using satellite ozone monitoring instrument NO<sub>2</sub> data and land use regression. *Environ Sci Technol* 2014; **4**: 2305–11.
- 53 Jamali S, Klingmyr D, Tagesson T. Global-scale patterns and trends in tropospheric NO<sub>2</sub> concentrations, 2005–2018. *Remote Sens (Basel)* 2020; **12**: 3526.
- 54 Qu Z, Henze DK, Cooper OR, Neu JL. Improving NO<sub>2</sub> and ozone simulations through global NO<sub>x</sub> emission inversions. *Atmos Chem Phys Discuss* 2020; published online April 8. <https://doi.org/10.5194/acp-2020-307> (preprint).
- 55 Hickman JE, Andela N, Tsigaridis K, Galy-Lacaux C, Ossouhou M, Bauer SE. Reductions in NO<sub>2</sub> burden over north equatorial Africa from decline in biomass burning in spite of growing fossil fuel use, 2005 to 2017. *Proc Natl Acad Sci USA* 2021; **118**: e2002579118.
- 56 Garcia E, Berhane KT, Islam T, et al. Association of changes in air quality with incident asthma in children in California, 1993-2014. *JAMA* 2019; **321**: 1906–15.
- 57 Barrington-Leigh C, Millard-Ball A. Global trends toward urban street-network sprawl. *Proc Natl Acad Sci USA* 2020; **117**: 1941–50.
- 58 GBD 2019 Diseases and Injuries Collaborators. Global burden of 369 diseases and injuries in 204 countries and territories, 1990–2019: a systematic analysis for the Global Burden of Disease Study 2019. *Lancet* 2020; **396**: 1204–22.
- 59 Keet CA, Matsui EC, McCormack MC, Peng RD. Urban residence, neighborhood poverty, race/ethnicity, and asthma morbidity among children on Medicaid. *J Allergy Clin Immunol* 2017; **140**: 822–27.